

# Role of dehydration catalyst acid properties on one-step DME synthesis over physical mixtures

F.S. Ramos<sup>a</sup>, A.M. Duarte de Farias<sup>b</sup>, L.E.P. Borges<sup>a</sup>,  
J.L. Monteiro<sup>c</sup>, M.A. Fraga<sup>b</sup>, E.F. Sousa-Aguiar<sup>d</sup>, L.G. Appel<sup>b,\*</sup>

<sup>a</sup> Instituto Militar de Engenharia, Praça General Tibúrcio, 80 Praia Vermelha, Rio de Janeiro 22290-270, Brazil

<sup>b</sup> Laboratório de Catálise, Instituto Nacional de Tecnologia/MCT, Av. Venezuela 82/507, Rio de Janeiro 22081-312, Brazil

<sup>c</sup> NUCAT/COPPE, Universidade Federal do Rio de Janeiro, Ilha do Fundão, C.P. 68502, Rio de Janeiro 21941, Brazil

<sup>d</sup> CENPES/Petrobras, Ilha do Fundão, Cidade Universitária, Quadra 7, Rio de Janeiro 21949-900, Brazil

Available online 7 March 2005

## Abstract

The direct synthesis of dimethyl ether (DME) was studied in a continuous high-pressure unit composed basically of a Berty reactor and on-line gas chromatograph. A commercial methanol synthesis catalyst and some solid-acid catalysts (alumina, HZSM-5, tungsten–zirconia and sulfated-zirconia) were used as physical mixtures. The dehydration catalysts were characterised by pyridine adsorption followed by IR spectroscopy and tested in the methanol dehydration reaction itself. All samples were active regardless of the differences in their acidity and a relationship between catalytic activity for methanol-to-DME and acidity could be envisaged; the activity of a solid acid on this reaction was found to be determined mainly by the number of its more acidic sites. On the one-step DME synthesis from syngas the addition of an acid catalyst to the catalytic system strongly shifted the methanol synthesis reaction, increasing significantly the pass conversion of CO. As a general rule, it could be concluded that the determining rate of DME direct synthesis is determined by the acid properties of the dehydrating catalyst, i.e., its acid strength and number of acid sites.

© 2004 Elsevier B.V. All rights reserved.

**Keywords:** Dimethyl ether; Methanol; Natural gas; Synthesis gas; Solid-acid catalysts

## 1. Introduction

Dimethyl ether (DME) is considered the fuel for 21st Century. It can be applied in diesel trucks, for power generation, in fuel cells and also replacing LPG as cooking gas. This last application is an important alternative for developing countries, like China, India and Brazil that need portable fuel (bottled) for people who live far from the facilities of the big cities [1,2]. It is also worth stressing that DME is a clean fuel, as it is non-toxic and burns without particulate emission.

DME can be synthesized from natural gas, coal and also from agriculture residues. Two processes have been claimed so far; the first uses traditional methanol synthesis followed by a dehydration step. The second needs a catalyst or a

mixture of catalysts capable of producing methanol and ether from synthesis gas in the same reactor. The latter approach is thermodynamically more favorable, being also an opportunity for the development of new processes [3,4].

Some research groups [5–7] tried to prepare bifunctional catalyst by getting together both dehydration and hydrogenation sites in the same catalyst. Considering that the best methanol catalyst is obtained through a hydrotalcite precursor, the association of this kind of structure with dehydration catalysts based on porous acid materials is not straightforward. Different preparation procedures have thus been evaluated in the literature. The best results were obtained with coprecipitation-deposition synthesis [7]. Basically, this procedure consists of adding a suspension of alumina or zeolites to another one containing the hydrotalcite precursor previously prepared by coprecipitation. Indeed, this catalyst could be considered as a mixture of Cu/ZnO/Al<sub>2</sub>O<sub>3</sub> and alumina or zeolites small particles.

\* Corresponding author.

E-mail address: [appel@uol.com.br](mailto:appel@uol.com.br) (L.G. Appel).

Some patents reports high DME yields using physical mixtures of the classical methanol catalyst and alumina or zeolites [8]. They mostly deal with activity and selectivity aspects given no reference about the catalysts features that should be considered essential to the synthesis. Likewise, there is only a few information in the scientific literature concerning the behavior of such systems as they have so far been focused on different approaches to obtain a bifunctional system. However, it should be mentioned that the role of both hydrogenation and dehydration sites on determining the overall reaction rate has been rarely considered to design a suitable catalyst. Therefore, the aim of this work is to compare the activity and selectivity of different physical mixtures, prepared with commercially available catalysts, in an attempt to identify the role of the catalyst acid properties for the direct synthesis of DME.

## 2. Experimental

Several physical mixtures composed of a methanol synthesis catalyst (ACZ) and some solid-acid catalysts were investigated. Only commercially available materials were taken and ACZ/acid catalyst ratio of one was kept constant in all experiments. Two different aluminas, a porous ( $\text{Al}_2\text{O}_3\text{-C}$ ) and a non-porous ( $\text{Al}_2\text{O}_3\text{-D}$ ), were used. The  $\text{Al}_2\text{O}_3\text{-D}$  was supplied by Degussa;  $\text{Al}_2\text{O}_3\text{-C}$  and a HZSM-5 sample ( $\text{SAR} = 40$ ) were provided by Petrobras. Two zirconia-based powders were also studied, basically a sulfated-zirconia ( $\text{S-ZrO}_2$ ) and a tungsten-zirconia ( $\text{W/ZrO}_2$ ), both supplied by MEL Chemicals. The specific surface areas of all solid-acid samples used are listed in Table 1.

Pyridine thermodesorption experiments followed by IR spectroscopy were conducted to probe the acid–base properties of the dehydration catalysts using a Nicolet Magna spectrophotometer. The spectra were recorded from thin (20 mg) self-supporting wafers. The samples were pre-treated at 500 °C for 1 h under vacuum, submitted to a stream of air for 30 min and finally exposed to high vacuum for 30 min ( $10^{-7}$  Torr). Pyridine was adsorbed at room temperature, at 10 Torr for 1 h. Spectra were collected after desorption at 25, 150, 250 and 350 °C for 1 h under high vacuum.

The bare acid-solid samples were firstly tested in the methanol dehydration reaction, which were performed in a

conventional system with flow micro-reactor, monitored by on-line gas chromatography, with flame ionization detector (FID). The solid-acid catalysts were pre-treated at 500 °C during 1 h under air at 30 mL min<sup>-1</sup>. After, they were purged with nitrogen and cooled up to 200 °C, temperature at which methanol was admitted to the reactor. The reaction proceeded under a methanol partial pressure of 14.4 kPa, which was introduced to the system through a saturator, using  $\text{N}_2$  flux (30 mL min<sup>-1</sup>). The catalysts samples mass varied in order to guarantee differential condition, allowing to calculate the methanol dehydration reaction rate [9].

The DME direct synthesis was carried over the physical mixtures composed of the methanol synthesis catalyst and the dehydration solid in a continuous unit composed basically of a Berty reactor (Autoclave Engineers, 50 mL of total volume) and a gas chromatograph connected in line (Varian CP-3800), equipped with both a thermal conductivity detector (TCD) and a FID.

The Berty reactor is an internal recycle gradientless reactor, equipped with a fixed basket to hold the catalyst and with a fan over the basket. The reactor was equipped with temperature control and pressure indication.

The feed gas flow was controlled by a mass flow meter (Brooks). The output stream and the reactor pressure were controlled by a micrometric valve. The effluent was then analyzed by gas chromatography. In order to prevent methanol and water condensation, the line between the reactor and the chromatograph injection valve, including the micrometric valve, was electric heated and kept at around 100 °C during the tests.

The catalysts physical mixture was reduced under  $\text{H}_2/\text{He}$  flow (5%  $\text{H}_2$ , 30 mL min<sup>-1</sup>), for 1 h at 250 °C. After reduction, the gas was changed for synthesis gas ( $\text{H}_2/\text{CO} = 1$ ) and the reaction conditions (24 mL min<sup>-1</sup>, 250 °C, 5 MPa) were adjusted. For the conditions used in this work, the steady state was achieved after 4 or 5 h of reaction.

Additional tests were carried out with different ACZ and HZSM-5 physical mixtures; basically distinct ACZ/HZSM-5 ratios, ranging from one to four, were evaluated.

The catalysts activities were evaluated based on the overall reaction rate and the products selectivities were calculated at the same CO conversion level, around 10%.

## 3. Results and discussion

### 3.1. Acid properties of the dehydration catalysts

The FTIR spectra of pyridine adsorbed on the solid-acid catalysts is depicted in Fig. 1. The absorption bands at 1450 cm<sup>-1</sup> ( $\nu_{19b}$ ), 1490 cm<sup>-1</sup> ( $\nu_{19a}$ ), 1575 cm<sup>-1</sup> ( $\nu_{8b}$ ), 1595 cm<sup>-1</sup>, 1613 cm<sup>-1</sup> ( $\nu_{8a}$ ) and a shoulder at 1620 cm<sup>-1</sup> presented in Fig. 1(A) are typically observed over alumina samples and are indicative of their Lewis acid sites [9,10]. On the other hand, the spectra shown in Fig. 1(B) are more complex exhibiting bands assigned to pyridine coordinated

Table 1

Specific surface area and catalytic activity in methanol dehydration of the solid-acid catalysts

Samples	$S_{\text{BET}}$ (m <sup>2</sup> g <sup>-1</sup> )	$r_{\text{MetOH}}$ (μmol s <sup>-1</sup> g <sup>-1</sup> )	$r_{\text{MetOH}}$ (μmol s <sup>-1</sup> m <sup>-2</sup> )
$\text{Al}_2\text{O}_3\text{-D}$	110	6.82	0.062
$\text{Al}_2\text{O}_3\text{-C}$	210	10.50	0.050
$\text{S-ZrO}_2$	143	19.31	0.135
$\text{W/ZrO}_2$	94	7.33	0.078
ZSM-5	341	89.34	0.262

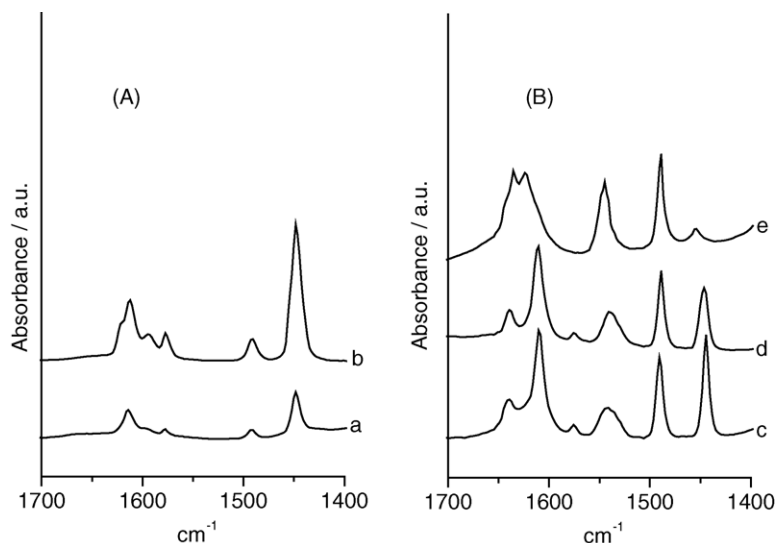


Fig. 1. Infrared spectra after pyridine adsorption and evacuation at 25 °C on: (A) Al<sub>2</sub>O<sub>3</sub>-D (spectrum a), Al<sub>2</sub>O<sub>3</sub>-C (spectrum b); (B) S-ZrO<sub>2</sub> (spectrum c), W/ZrO<sub>2</sub> (spectrum d), HZSM-5 (spectrum e).

on Lewis acid sites (1450, 1490 and 1610 cm<sup>-1</sup>) and to pyridinium ion bonded to Brönsted acid sites (1490, 1540 and 1640 cm<sup>-1</sup>). Indeed, Lewis and Brönsted acidity are usually present on HZSM-5 [10,11], medium-high sulfate loadings S-ZrO<sub>2</sub> [12,13] and tungsten-zirconia solids [14,15].

Fig. 2 presents the evolution of the intensities of pyridine 19b vibrational modes corresponding to both Lewis (1450 cm<sup>-1</sup>) and Brönsted (1540 cm<sup>-1</sup>) acid sites, normalised by surface area and wafer mass, as a function of desorption temperature. The data calculated at low temperature concerning alumina samples (Fig. 2A) reveal that Al<sub>2</sub>O<sub>3</sub>-C has a higher number of Lewis acid sites compared to Al<sub>2</sub>O<sub>3</sub>-D. However, it can be seen that the strength of these acid sites on both samples is quite equivalent as the pyridine thermodesorption follows the same pattern. As for HZSM-5 and the zirconia-based solids, it was found that

they roughly present the same number of Lewis acid sites; their acidity strength is rather distinct though. The sulfate-doped zirconia has the more acidic Lewis sites since its absorption band intensity decreases more slowly upon outgassing than for the other samples.

Even though these three last samples feature Lewis acidity, it has been known that their Brönsted sites are usually the responsible for their role in acid-catalysed reactions. The Lewis sites on zirconia-based samples, for instance, resemble those from bare zirconia since the addition of either sulfate groups or dispersed tungsten species are credited with generating Brönsted acid sites [12–17]. Hence, their Brönsted acidity distribution is also presented in Fig. 2(B). It clearly shows that the amount of Brönsted centres of HZSM-5 is large compared to the zirconia-based samples. Additionally, it can be seen that its acidic strength is far more significant.

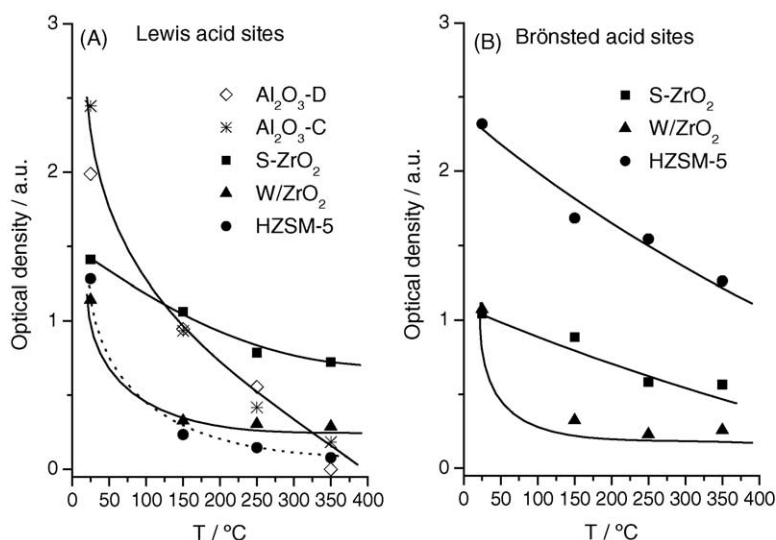


Fig. 2. Acid strength distribution as a function of the pyridine desorption temperature of all the studied solid-acid samples.

### 3.2. Methanol dehydration

Methanol dehydration was carried out at atmospheric pressure over pure solid-acid catalysts. The reaction rates were calculated at 200 °C under differential conditions and the values are collected in Table 1. It must be noted that those systems were totally selective to dimethyl ether under such reaction conditions.

Several reaction mechanisms have been presented for methanol dehydration on acid catalysts [3,18,19]. Either Brönsted acid sites or Lewis acid–base pair sites are believed to play a role in such reaction and, generally, the stronger the acid sites the more active the catalysts. However, it should be recalled that as far as Brönsted sites are involved, their strength and the reaction temperature should be controlled to avoid hydrocarbons formation. The mechanism based on Lewis acidity, on the other hand, requires an adjacent acid–base pair sites to provide the reaction between the adsorbed alcohol molecule on an acidic site and an adsorbed alkoxide anion on a basic site [18,19]. The results compiled in Table 1 show that all samples were indeed active regardless of the differences in their acidity. A relationship between catalytic activity for methanol-to-DME and acidity can be easily envisaged. The fairly identical Lewis acidity distribution determined for aluminas samples (Fig. 2a) may, thus, be responsible for a quite similar catalytic behaviour on methanol dehydration as shown in Table 1. Likewise, a straightforward correlation may also be found when Brönsted acidity is considered for the other samples. Fig. 3 presents the catalytic activity as a function of both total and more acidic Brönsted acid sites. The density of the more acidic sites was estimated taking into account the infrared spectroscopic data obtained after pyridine desorption at 250 °C. It is seen that the attempt to correlate the dehydration rate and total acid sites fails to give a satisfactory result. Nevertheless, the values can be perfectly correlated with the density of strong acid sites, indicating that the activity of a solid acid on this reaction is determined

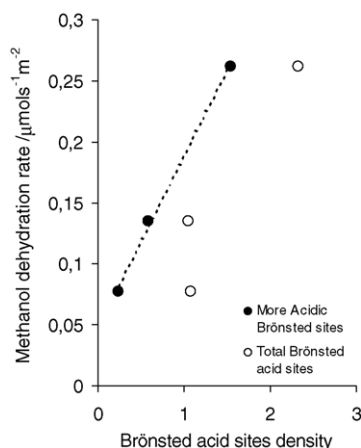
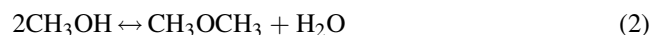


Fig. 3. Correlation between Brönsted acidity and methanol dehydration rate.

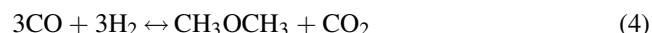
mainly by the number of its more acidic sites. Yet, one could suppose that the ZrO<sub>2</sub>-based catalysts might also react based on their Lewis acid–base pair sites. Indeed, besides the acid sites, Lewis basic centres can also be detected on ZrO<sub>2</sub> surface as observed in our laboratory. However, we also verified that the activity of bare ZrO<sub>2</sub> in methanol dehydration is extremely low. Therefore, it can be inferred that the contribution of such sites is negligible when compared with the Brönsted acid centres.

### 3.3. Direct DME synthesis

Direct DME synthesis was evaluated based on the CO consumption rates and the products selectivities. Fig. 4 displays the activity values obtained from all physical mixtures studied. The commercial methanol catalyst (ACZ) is also included to be taken as a reference. It is clear that the CO consumption increases considerably by adding a dehydrating catalyst. Such trend is expected as the direct synthesis of DME from syngas proceeds basically through three reaction steps, namely methanol synthesis (reaction (1)), methanol dehydration (reaction (2)) and the water gas shift reaction (reaction (3)):



The presence of an acid catalyst removes the methanol formed by reaction (1) shifting the overall reaction (4) toward the right-hand side.



One could thus expect that the higher the methanol dehydration rate is, the higher the CO consumption rate will be. However, comparing the direct synthesis activities calculated for the mixtures displayed in Fig. 4 with the solid-acid catalysts performances listed in Table 1, it can be seen that they do not follow the same sequence. Despite the

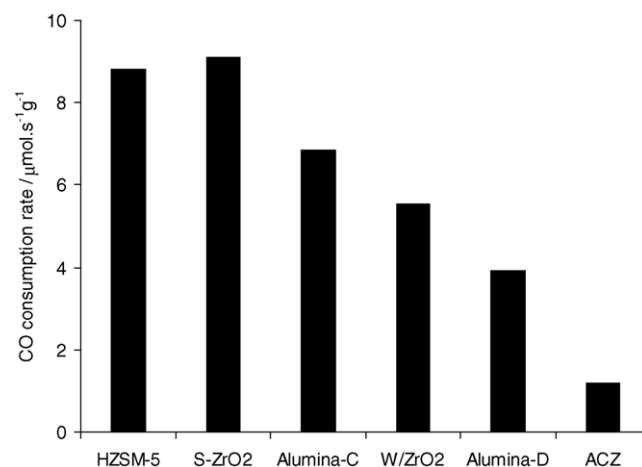


Fig. 4. CO consumption rate of the admixed catalysts of ACZ and dehydration catalysts. CO<sub>2</sub> formation was not considered for the rate calculation.

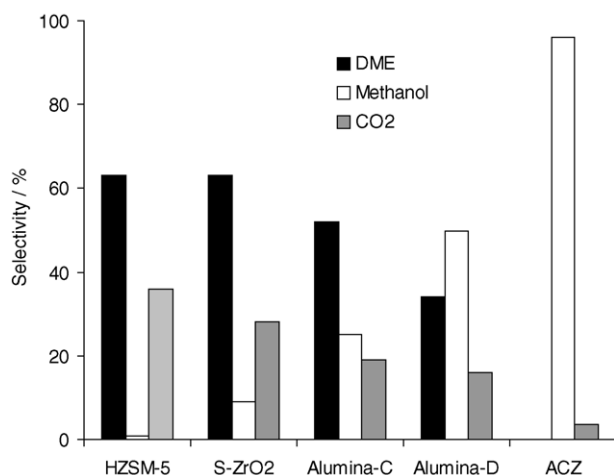


Fig. 5. Selectivities towards DME, methanol and CO<sub>2</sub> for ACZ and dehydration catalysts physical mixtures.

dramatic difference between HZSM-5 and S-ZrO<sub>2</sub> behaviours for dehydrating methanol (Table 1), the performances of the admixed catalysts of ACZ and such solids are equivalent, allowing the conclusion that the overall reaction rate is determined by the methanol synthesis step (reaction (1)) rather than the DME formation itself (reaction (2)). The other mixtures prepared with ACZ and aluminas (either D or C) or tungsten–zirconia exhibited different patterns. For these samples, the values of the DME direct synthesis activity are in relatively good agreement with their corresponding solid-acid behaviour, especially when the dehydration rate is calculated on the same base, i.e., per catalyst mass unit (Table 1). Therefore, it can be inferred that, in these cases, the methanol dehydration rate controls the DME production.

The selectivities obtained with all samples corroborate the activity discussion above. It may be noted in Fig. 5 that the selectivities towards methanol and DME follow opposite trends. DME selectivity is lower over the less active mixtures while an equivalent production is achieved over both HZSM-5 and sulfated-zirconia, which further confirms that methanol is not efficiently dehydrated over weak acidic solids. A quite significant CO<sub>2</sub> production must also be noticed over all systems. Besides, it should be observed that the CO<sub>2</sub> selectivity seems to follow the DME formation. As a matter of fact, CO<sub>2</sub> is formed through the water gas shift reaction (reaction (3)), which proceeds along with the alcohol dehydration reaction due to the water formation (reaction (2)).

The mixture containing methanol catalyst and HZSM-5 has thus been found to be one of the most effective amongst the systems evaluated so far. Additional tests were carried out with mixtures of different compositions, in which lower amounts of HZSM-5 were used. As shown in Fig. 6, the reaction data remain essentially unchanged within the whole ACZ/HZSM-5 ratio studied. These findings provide further evidences that over such mixtures the reaction is controlled by the methanol synthesis step.

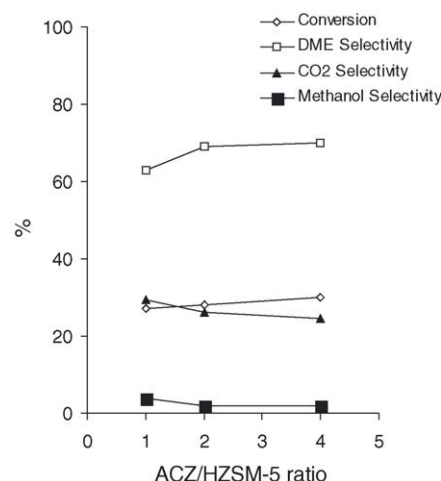


Fig. 6. DME, methanol and CO<sub>2</sub> selectivity and conversion for ACZ and HZSM-5 physical mixtures with different compositions.

The above-presented results provide important information for choosing solid catalysts to compose a hybrid system for the direct synthesis of DME from syngas. As far as an efficient catalyst for methanol synthesis is available the DME production may be effectively achieved by adding an optimised amount of a solid-acid catalyst.

#### 4. Conclusion

One-step DME synthesis from syngas can be achieved over physical mixture of a classic methanol catalyst and a solid-acid catalyst. The activity of a solid acid on the methanol dehydration reaction was found to be determined mainly by the number of its more acidic sites. The presence of such acid catalyst to the catalytic system strongly shifts the methanol synthesis reaction, increasing significantly the pass conversion of CO. As a general rule, it can be concluded that the determining rate of DME direct synthesis is determined by the acid properties of the dehydrating catalyst, i.e., its acid strength and number of acid sites.

#### Acknowledgments

The authors are indebted to Ms. Angela M. Lavogade Esteves and Ms. Magali Almeida Farias for their assistance in the experimental work. Degussa and MEL Chemicals are gratefully acknowledged for kindly providing the solid-acid samples. The financial support of FINEP is also acknowledged.

#### References

- [1] J.H. Lunsford, Catal. Today 63 (2000) 165.
- [2] S.C. Sorenson, J. Eng. Gas Turbines Power 123 (2001) 653.

- [3] M. Xu, J.H. Lunsford, D.W. Goodman, A. Battacharyya, *Appl. Catal. A* 149 (1997) 289.
- [4] Y. Adachia, M. Komotob, I. Watanabec, Y. Ohnoc, K. Fujimotoa, *Fuel* 79 (2000) 229.
- [5] Q. Ge, Y. Huang, F. Qiu, S. Li, *Appl. Catal. A* 167 (1998) 23.
- [6] T. Shikada, Y. Ohno, T. Ogawa, M. Mizuguchi, M. Ono, K. Fujimoto, US Patent 6,147,125 (2000).
- [7] K. Sun, W. Lu, F. Qiu, S. Liu, X. Xu, *Appl. Catal. A* 252 (2003) 243.
- [8] X.D. Peng, G.E. Parris, B.A. Toseland, P.G. Battavio, US Patent 5,753,716 (1998).
- [9] A.M. Duarte de Farias, A.M.L. Esteves, F. Ziarelli, S. Caldarelli, M.A. Fraga, L.G. Appel, *Appl. Surf. Sci.* 227 (2004) 132.
- [10] G. Busca, *Catal. Today* 41 (1998) 191.
- [11] Y. Sun, S.M. Campbell, J.H. Lunsford, G.E. Lewis, D. Palke, L.M. Tau, *Catal. Today* 143 (1993) 32.
- [12] C. Morterra, G. Cerrato, C. Emanuel, V. Bolis, *J. Catal.* 142 (1993) 349.
- [13] A. Patel, G. Coudurier, N. Essayem, J.C. Védrine, *J. Chem. Soc., Faraday Trans.* 93 (1997) 347.
- [14] D.G. Barton, S.L. Soled, E. Iglesia, *Top. Catal.* 6 (1998) 87.
- [15] C.D. Baertsch, S.L. Soled, E. Iglesia, *J. Phys. Chem. B* 105 (2001) 1320.
- [16] X. Song, A. Sayari, *Catal. Rev. – Sci. Eng.* 38 (1996) 329.
- [17] M. Scheithauer, R.K. Grasselli, H. Knözinger, *Langmuir* 14 (1998) 3019.
- [18] H. Knözinger, K. Kochloeft, W. Meye, *J. Catal.* 28 (1973) 69.
- [19] H. Knözinger, D. Dautzenberg, *J. Catal.* 3 (1974) 142.